The role of the choroid plexus in neutrophil invasion after traumatic brain injury

Joanna Szmydynger-Chodobska[1], **Nathalie Strazielle**[2], **Brian J. Zink**[1], **Jean-François Ghersi-Egea**[3], and **Adam Chodobski**[1]

[1] Department of Emergency Medicine, The Warren Alpert Medical School of Brown University, Providence, RI 02903, USA

[2] Brain-I, Lyon, France

[3] INSERM U842, Université de Lyon, Lyon1, Faculté de Médecine Laennec, 69372 Lyon, France

Abstract

Traumatic brain injury (TBI) frequently results in neuroinflammation, which includes the invasion of neutrophils. After TBI, neutrophils infiltrate the choroid plexus (CP), a site of the blood-cerebrospinal fluid (CSF) barrier (BCSFB), and accumulate in the CSF space near the injury, from where these inflammatory cells may migrate to brain parenchyma. We have hypothesized that the CP functions as an entry point for neutrophils to invade the injured brain. Using the controlled cortical impact model of TBI in rats and an *in vitro* model of the BCSFB, we show that the CP produces CXC chemokines, such as cytokine-induced neutrophil chemoattractant (CINC)-1 or CXCL1, CINC-2α or CXCL3, and CINC-3 or CXCL2. These chemokines are secreted both apically and basolaterally from choroidal epithelium, a prerequisite for neutrophil migration across epithelial barriers. Consistent with these findings, we also provide electron microscopic evidence that neutrophils infiltrate the choroidal stroma and subsequently reach the intercellular space between choroidal epithelial cells. This is the first detailed analysis of the BCSFB function related to neutrophil trafficking. Our observations support the role of this barrier in post-traumatic neutrophil invasion.

Keywords

blood-cerebrospinal fluid barrier; choroid plexus; CXC chemokines; neutrophils; traumatic brain injury

Introduction

Choroid plexus (CP) is located in all four cerebral ventricles. It is a highly vascularized tissue, in which blood microvessels are enclosed by a single layer of cuboidal epithelial cells (Strazielle and Ghersi-Egea, 2000). The CP is the major source of cerebrospinal fluid (CSF); however, together with the arachnoid membrane, it also constitutes the blood-CSF barrier (BCSFB). Increasing evidence indicates that the BCSFB plays an important role in brain immune response and neuroinflammation (Strazielle and Ghersi-Egea, 2000). Choroidal venules have been demonstrated to express P- and E-selectins, and it has been proposed that

the BCSFB is involved in the recruitment of T cells to the CSF (Kivisäkk *et al*, 2003). We, along with other researchers, have shown that, after traumatic brain injury (TBI), neutrophils infiltrate the lateral ventricle CP and accumulate in the cistern of velum interpositum, a part of the 3rd ventricle, and in the subarachnoid CSF space near the injury site, from where these inflammatory cells appear to migrate to traumatized brain parenchyma (Carlos *et al*, 1997; Chodobski *et al*, 2003). These findings suggested that not only the blood-brain barrier (BBB), but also the BCSFB and CSF pathways are involved in neutrophil invasion observed after TBI. Neutrophil invasion has been shown to contribute to the formation of post-traumatic brain edema (Schoettle *et al*, 1990), and treatments directed to counter neutrophil influx to the injured brain exhibited several beneficial effects (Matsumoto *et al*, 1997; Yamasaki *et al*, 1997; Beech *et al*, 2001).

The accumulation of neutrophils in the CP occurring after injury indicated that the choroidal tissue has the ability to produce neutrophil chemoattractants; however, such properties of the CP have not yet been investigated. Neutrophil chemoattractants belong to the family of CXC chemokines (Kobayashi, 2008). Cytokine-induced neutrophil chemoattractant (CINC)-1 (referred to as CXCL1), CINC-2α and CINC-2β (both referred to as CXCL3), and CINC-3 (also known as macrophage inflammatory protein-2 or MIP-2; referred to as CXCL2) are the four major rat chemokines that possess neutrophil chemotactic activity (Huang *et al*, 1992a, b; Nakagawa *et al*, 1994). Various types of epithelial cells have previously been shown to synthesize CXC chemokines upon exposure to proinflammatory cytokines, such as tumor necrosis factor-α (TNF-α) and interleukin-1β (IL-1β) (Takaishi *et al*, 2000; Handa *et al*, 2004). It has also been demonstrated that both basolateral and apical secretion of chemokines is necessary to promote transepithelial migration of neutrophils (McCormick *et al*, 1995, 1998). The aim of this study was to define a role of the CP in neutrophil recruitment to the injured brain. Accordingly, we characterized the ability of the CP to produce CXC chemokines in response to injury using a rat model of TBI and determined the direction of cytokine-dependent release of these chemokines (across the apical vs. basolateral membrane of choroidal epithelium) using an *in vitro* model of the BCSFB. We also used transmission electron microscopy (TEM) to demonstrate neutrophil trafficking across the BCSFB.

Materials and methods

Reagents and antibodies

ThermoScript RNase H⁻ reverse transcriptase and RNase inhibitor, RNaseOut, were obtained from Invitrogen (Carlsbad, CA, USA). HotStart *Taq* DNA polymerase was purchased from Qiagen (Valencia, CA, USA). Low-endotoxin bovine serum albumin (BSA; A2058) was from Sigma (St Louis, MO, USA) and laminin was from Becton Dickinson (Bedford, MA, USA). Recombinant rat IL-1β and CINC-1 were obtained from R&D Systems Europe (Lille, France) and PeproTech (Paris, France), respectively. ^{14}C-sucrose was from Amersham (Little Chalfont, UK). Rabbit polyclonal antibodies to rat CINC-1 and rat IL-1β were from Antigenix America (Huntington Station, NY, USA), whereas rabbit anti-human myeloperoxidase (MPO) antibody was from Dako (Glostrup, Denmark). Rabbit polyclonal antibody to rat Na^+-K^+-$2Cl^-$ co-transporter 1 (NKCC1) was obtained from Chemicon International (Temecula, CA, USA). The following mouse monoclonal antibodies were used: anti-rat TNF-α (clone 45418) from R&D Systems, anti-rat CD11b (clone MRC OX-42) from Serotec (Oxford, UK), anti-mouse β-catenin (clone 14) from BD-Transduction Labs (Lexington, KY, USA), and anti-rat Golgi 58K protein (clone 58K-9) from Sigma. Secondary antibodies were obtained from Molecular Probes (Eugene, OR, USA). These were goat anti-rabbit and anti-mouse IgGs conjugated with Alexa 488 or Alexa 594.

The rat TBI model

Adult male Long-Evans rats weighing 250–350 g (Harlan, Indianapolis, IN, USA) were used for gene expression analysis, whereas adult male Sprague-Dawley rats (Charles River, MA, USA) of the same weight were used for other studies. They were kept at 22°C on a 12-h light cycle and maintained on standard pelleted rat chow and water *ad libitum*. The surgical and animal care procedures were in accordance with the guidelines of the Animal Care and Use Committee of Rhode Island Hospital and conformed to international guidelines on the ethical use of animals. Rats were anesthetized with intraperitoneal pentobarbital sodium (60 mg/kg). Rectal temperature was continuously monitored and maintained at ~37°C. The animals were placed in a stereotactic frame, and before the incision, the scalp was infiltrated with 2% lidocaine solution. A 4-mm craniotomy was performed on the right side of the skull to expose the dura, with the center of the opening located 3 mm posterior to bregma and 2.5 mm lateral to the midline. TBI was produced using a controlled cortical impact device obtained from Grzegorz Micha owski (Michalowski Inc., Zossen, Germany). The velocity of impact was 5 m/sec and the duration of impact was 50 msec. The diameter of impactor's tip was 2.5 mm and the depth of brain deformation was set at 3 mm. Immediately after the insult, the scalp was closed with a nylon suture and the rats were allowed to recover in their cages. In sham-injured animals, the same surgical procedures were performed, but the injury was not produced.

Real-time reverse-transcriptase polymerase chain reaction (RT-PCR)

At 1, 2, 4, and 6 h, and 1, 2, and 4 days after TBI, rats (9–10 animals per time point) were re-anesthetized with pentobarbital sodium. Samples of the lateral ventricle CP, both ipsilateral and contralateral to injury, were collected separately and pooled into three subgroups (3–4 rats per subgroup). Samples of the cerebral cortex adjacent to the lesion and those of the contralateral cortex from the corresponding region were collected. Samples of the lateral ventricle CP and those of the cerebral cortex were also collected from sham-injured rats. Total RNA was isolated using NucleoSpin RNA II kit (Macherey-Nagel, Düren, Germany). First-strand cDNAs were synthesized using oligo(dT)$_{20}$ primer (50 pmol) and 15 U of ThermoScript RNase H$^-$ reverse transcriptase. Forty units of RNase inhibitor, RNaseOut, were also added to the reverse transcription reactions. For each reaction, 0.5 μg of total RNA was used and the reactions were carried out for 1 h at 50°C.

Real-time PCR was performed using the TaqMan chemistry in a DNA Engine Opticon System (MJ Research, Waltham, MA, USA). The sequences of primers and TaqMan probes, and the predicted sizes of PCR products are given in Table 1. Cyclophilin A was used for the normalization of obtained data. The 50-μl PCR reaction mixtures contained 0.2 mM mixed dNTPs, 0.2 μM each primer, 0.1 μM TaqMan probe, 5 mM MgCl$_2$, 1 U HotStart *Taq* DNA polymerase, and 1/20 of the reverse transcription reaction product. For cyclophilin A, 1/2000 of the reverse transcription reaction product was used. The reaction mixtures were heated to 95°C for 15 min and were then subjected to 40 cycles of denaturation (94°C, 15 sec) and annealing/extension (60°C, 45 sec). The results are presented as a number of copies of mRNA for the gene of interest per 100 copies of mRNA for cyclophilin A.

Immunohistochemistry

Rats (2–4 animals per group) were re-anesthetized with pentobarbital sodium and were perfused transcardially with ice-cold 0.9% NaCl, followed by ice-cold 4% paraformaldehyde in 0.05 M phosphate-buffered saline (PBS), pH 7.4. Brains were removed and post-fixed for additional 4 h in the paraformaldehyde/PBS solution at 4°C. They were then incubated overnight in 20% sucrose in PBS and embedded in Tissue-Tek OCT compound (Sakura Finetek, Torrance, CA, USA). Coronal brain sections were cut on a cryostat at 10 μm.

Immunohistochemical procedures were performed at room temperature, except for the incubation with primary antibodies that was completed at 4°C. All incubations were performed in PBS containing 0.25% BSA and 0.25% Triton X-100 (TX-100). For washes, PBS containing 0.1% BSA and 0.1% TX-100 was used. To minimize non-specific staining, the brain sections were incubated for 30 min with 10% normal goat serum (Jackson Immunoresearch Labs, West Grove, PA, USA). Four percent of normal goat serum was also added when the sections were incubated with primary and secondary antibodies. After the initial blocking step, the brain sections were incubated overnight with primary antibodies. The following concentrations of primary antibodies were used: 1 μg/ml for CINC-1 and IL-1β, 5 μg/ml for TNF-α, 13.2 μg/ml for MPO, 0.4 mg/ml for Golgi 58K protein, 2 μg/ml for CD11b, 10 μg/ml for NKCC1, and 2.5 μg/ml for β-catenin. Six 10-min washes were then performed and the sections were incubated for 1 h with secondary antibodies at a concentration of 2 μg/ml. After four 10-min washes, the brain sections were mounted with Vectashield mounting medium (Vector Labs, Burlingame, CA, USA).

Myeloperoxidase (MPO) activity assay

To quantitatively assess the magnitude of post-traumatic accumulation of neutrophils in choroidal tissue, the MPO activity assays were performed. Rats (4 animals per group) were re-anesthetized with pentobarbital sodium and were perfused transcardially with ice-cold 0.9% NaCl. Samples of the lateral ventricle CP, both ipsilateral and contralateral to injury, those of the cerebral cortex adjacent to the lesion, and those of the contralateral cortex from the corresponding region, were collected. They were homogenized at room temperature in 50 mM potassium phosphate buffer (PPB), pH 6.0, and centrifuged for 20 min at 60,000×g at 4°C. After centrifugation, the pallet was washed in PPB to remove the inhibitors of MPO activity and was resuspended in 0.5% hexadecyltrimethylammonium bromide in PPB to liberate MPO from neutrophilic granules. Samples were then centrifuged for 15 min at 15,000×g and portion of supernatant was added to PPB containing *o*-dianisidine dihydrochloride (0.2 mg/ml) and 0.001% H_2O_2. Changes in absorbance at 460 nm were assayed spectrophotometrically. One unit of MPO activity was defined as the degradation of 1 μmol of H_2O_2 per min. Results are expressed as units of MPO activity per gram of tissue.

TEM analysis

At 1 day after TBI or sham injury, rats (2–6 animals per group) were re-anesthetized with pentobarbital sodium and the samples of the lateral ventricle CP, both ipsilateral and contralateral to injury, were removed and fixed overnight in 2.5% glutaraldehyde in 0.15 M sodium cacodylate buffer, pH 7.4, at 4°C. Following fixation, the specimens were treated with 1% OsO_4 in cacodylate buffer for 1 h at 4°C. They were then dehydrated in a graded acetone series and embedded in Epox 812 resin (Fullam, Latham, NY, USA). Ultrathin sections (50–60 nm) were prepared, retrieved onto 300 mesh copper grids, and contrasted with uranyl acetate and lead citrate. Sections were examined using a Morgagni 268 transmission electron microscope (FEI, Hillsboro, OR, USA).

Primary cell cultures of rat choroidal epithelial cells

The procedures were conducted according to the guidelines approved by the French Ethical Committee (decree 87–848) and by the European Community directive 86–609-EEC. Animals were obtained from Harlan (Gannat, France). Choroidal epithelial cells were isolated as previously described (Strazielle and Ghersi-Egea, 1999) and were seeded on Transwell Clear inserts (Costar, Cambridge, MA, USA) with the pore size of 0.4 μm pre-coated with laminin. The cells were kept at 37°C in a humidified atmosphere of 5% CO_2/95% air and were fed every other day with medium containing 10% fetal bovine serum. The experiments were performed 5 days after the cells reached confluence.

Secretion of CINC-1

The cells were serum starved in serum-free medium (SFM) supplemented with 0.1% BSA for 24 h prior to experimentation. On the day of experiment, BSA-containing SFM was renewed in both chambers and cytokine treatment was initiated by exposing the apical surface of the cell monolayers to various concentrations of rat IL-1β for different periods of time. In time-course studies, the cells were incubated with 0.1 ng/ml of IL-1β for 1.5, 4, 8, and 24 h. In dose-response studies, the cells were exposed to 0.01, 0.1, 1, and 10 ng/ml of IL-1β for 8 h. Control monolayers (incubated in SFM without IL-1β) were processed simultaneously. At the end of the incubation periods, media were collected from the apical and basolateral chambers and stored at −80°C until further processing for CINC-1 quantification. The epithelial monolayers were subsequently analyzed for possible changes in paracellular permeability. The concentration of CINC-1 in the culture media was determined by ELISA using the Quantikine Rat CINC-1 Immunoassay kit from R&D Systems. The samples were assayed in duplicates after appropriate dilution.

Basolateral-to-apical permeability to CINC-1

Cells were serum starved as described above and their basolateral surface was exposed to either recombinant CINC-1 (0.4 or 4 ng/ml) or conditioned media collected from basolateral chambers in another set of epithelial cell monolayers treated for 4 h with 0.1 ng/ml of IL-1β. After 1.5 and 4 h of incubation, media were sampled from both compartments to assess the CINC-1 concentration. No degradation of recombinant or endogenous (conditioned media) CINC-1 during the incubation periods was observed.

Measurement of paracellular permeability of epithelial monolayers

The integrity of epithelial monolayers was examined by measuring the permeability of each filter to the paracellular permeability marker, ^{14}C-sucrose. The permeability $\times$ surface area product, PSt, was calculated from the ^{14}C-sucrose clearance rates as previously described (Strazielle and Preston, 2003). The permeability coefficient, Pt, was calculated by dividing PSt by the surface area of the cell monolayer.

Statistical analysis

For statistical evaluation of data, ANOVA was used, followed by the multiple comparison tests, as described in figure legends. *P*<0.05 was considered statistically significant.

Results

Post-traumatic increase in mRNA for proinflammatory cytokines and CXC chemokines in choroidal tissue and the injured cortex

The CP is not only a target for proinflammatory cytokines, such as TNF-α and IL-1β (Ericsson *et al*, 1995; Nadeau and Rivest, 1999), but is also a site of their synthesis (Quan *et al*, 1999). Accordingly, we first examined post-traumatic changes in choroidal expression of TNF-α and IL-1β using real-time RT-PCR. Trauma resulted in biphasic changes in TNF-α expression in the ipsilateral CP. Compared with sham-injured rats, there was a rapid (within 1 h post-TBI) increase in TNF-α mRNA, followed by a gradual decrease and a secondary increase at 6 h after TBI (Figure 1A). Interestingly, we also observed an increase in TNF-α expression in the contralateral CP at 1 h post-TBI, but not at later time points after injury. The levels of TNF-α expression in the injured cortex were slightly higher than those found in the CP (Figure 1C). The time course of post-traumatic changes in TNF-α mRNA was similar to that found in the CP, except that the secondary increase in mRNA levels at 6 h post-TBI was not observed. No changes in TNF-α expression in the contralateral cortex were observed. The time course of changes in choroidal IL-1β expression differed from that found for TNF-α. The message for

IL-1β in the ipsilateral CP increased gradually after injury to reach a peak at 6 h post-TBI (Figure 1B). The synthesis of IL-1β in the contralateral CP was also upregulated at 4 and 6 h after TBI compared to sham injury; however, the levels of mRNA for IL-1β found in the contralateral CP were significantly lower than those observed in the ipsilateral tissue. The levels of IL-1β mRNA in the injured cortex were higher than those found in the ipsilateral CP (Figure 1D); however, no changes in IL-1β expression in the contralateral cortex were observed.

Post-traumatic changes in choroidal expression of three neutrophil chemoattractants, CINC-1, CINC-2α, and CINC-3/MIP-2, were examined. The expression levels of CINC-2β were found to be low (data not shown). The maximum increase in mRNA for all three chemokines in the ipsilateral CP was observed at 6 h after TBI, with the levels of chemokine synthesis being 120–430-fold higher compared to those found in sham-injured animals (Figures 2A–2C). The expression of CINC-2α in the contralateral CP was also upregulated at 4 and 6 h post-TBI and that of CINC-3/MIP-2 tended to increase during the same period of time after injury; however, the levels of mRNA for these chemokines found in the contralateral CP at 6 h post-TBI were significantly lower than those observed in the ipsilateral CP. By contrast, the induction of CINC-1 synthesis was limited to the ipsilateral CP. The peak in expression of CINC-1 and other CXC chemokines (observed at 6 h post-TBI) was followed by an abrupt decrease at 1 day after trauma and the levels of chemokine expression remained low until the end of the 4-day observation period. The levels and the time course of changes in expression of these chemokines in the injured cortex were similar to those found in the CP, but the upregulation of chemokine synthesis in the contralateral cortex was not observed at any time point post-TBI (Figures 2D–2F).

Choroidal expression of proinflammatory cytokines and CINC-1 at the protein level

The immunohistochemical analysis of choroidal tissue harvested at 8 h post-TBI showed the TNF-α-positive staining of epithelial cells in the ipsilateral CP (Figure 3A). Co-localization of this staining with the immunostaining for the NKCC1 co-transporter, an integral membrane protein expressed apically in choroidal epithelium (Praetorius and Nielsen, 2006), suggested that this TNF-α-immunoreactive product represents the transmembrane precursor form of TNF-α (Kriegler *et al*, 1988). No TNF-α-immunopositive staining was observed in the contralateral CP (data not shown). In the ipsilateral CP, IL-1β was highly expressed in epiplexus (Kolmer) cells (Ling *et al*, 1998), but not in stromal macrophages (Figure 3B). In the contralateral CP, the epiplexus cells were negative for IL-1β (data not shown). Interestingly, IL-1β also appeared to be constitutively expressed in choroidal epithelium (Figure 3C). The IL-1β-immunoreactive product was associated with the Golgi complex, as demonstrated by double immunostaining with monoclonal antibody to the Golgi marker, Golgi 58K (Bloom and Brashear, 1989), and was found in both the ipsilateral and contralateral CPs, as well as in the CP from sham-injured rats (data not shown). Intense cytoplasmic CINC-1-positive staining of epithelial cells in the ipsilateral, but not in contralateral, CP was also associated with the Golgi complex (Figure 3D). The localization of CINC-1 to the Golgi complex is in line with increased synthesis of this secreted protein occurring after TBI. In addition, the CINC-1-immunopositive staining was localized to the basolateral membrane of choroidal epithelial cells (Figure 3E), and this pattern of staining was similar to that found for ion transporters expressed basolaterally in the choroidal epithelium (Praetorius and Nielsen, 2006). The basolateral CINC-1-positive staining did not co-localize with the staining for β-catenin, a component of the adherens junction complex, indicating that CINC-1 is confined to a part of the basolateral membrane that is distinct from areas occupied by adherens junctions (Figures 3E and 3H). Since chemokines have the ability to bind to heparan sulfates (Kuschert *et al*, 1999), it is possible that the basolateral localization of CINC-1 was associated with the binding of this secreted protein to heparan sulfate proteoglycans expressed on the basolateral surface of choroidal epithelium (Fayein *et al*, 1992; Snow *et al*, 1994). The levels of CINC-1 expression

varied in choroidal tissue with some epithelial cells showing strong CINC-1-immunopositive staining and others bearing weaker CINC-1 immunoreactivity. These variable levels of CINC-1 expression appeared to result in uneven distribution of neutrophils infiltrating the choroidal tissue observed after injury (data not shown). Double immunostaining for CINC-1 and NKCC1 showed that the CINC-1-immunoreactive product is not associated with the apical membrane domain (data not shown). In the contralateral CP, only a weak basolateral staining for CINC-1 was observed (Figure 3F). This pattern of staining was similar to that found in the choroidal tissue collected from sham-injured animals (data not shown).

Polarity of CINC-1 secretion by the choroidal epithelium

To test whether IL-1β induces CINC-1 synthesis in the choroidal epithelium and to determine the direction of CINC-1 release (across the apical vs. basolateral membrane), we used an *in vitro* polarized model of the rat BCSFB, which reproduces the *in vivo* properties of choroidal epithelium (Strazielle and Ghersi-Egea, 1999). The type I IL-1 receptor has previously been identified by *in situ* hybridization to be expressed in the CP (Ericsson *et al*, 1995), and we confirmed its expression on epithelial monolayers forming the *in vitro* BCSFB (data not shown). Previous studies of neurotrauma patients have shown that not only the CSF, but also the plasma levels of proinflammatory cytokines are elevated after injury (Singhal *et al*, 2002; Magnoni *et al*, 2003; Buttram *et al*, 2007). Therefore, in preliminary studies, either the apical (CSF-facing) or basolateral (stroma/blood-facing) surface of epithelial monolayers was exposed to IL-1β (10 ng/ml) and CINC-1 secretion was monitored for 24 h. Since the similar amounts of CINC-1 were produced with the apical and basolateral exposures to IL-1β, in subsequent experiments, this cytokine was only applied to the apical chamber.

Under control conditions, CINC-1 was constitutively produced, but it was barely detectable, and the total amount of CINC-1 secreted to the apical and basolateral chambers during the 24-h observation period was ~7 pg/filter. This secretion was polarized, with CINC-1 being largely released across the apical membrane. In time-course studies, the cells were incubated with 0.1 ng/ml of IL-1β for 1.5, 4, 8, and 24 h (Figure 4A). At this concentration of IL-1β, CINC-1 secretion was predominantly basolateral throughout the 24-h observation period. During the initial 4-h period of exposure to IL-1β, the CINC-1 levels in the apical and basolateral chambers increased rapidly. However, between 4 and 8 h of incubation with this cytokine, the CINC-1 levels increased at a much slower rate, and the concentrations of CINC-1 in both the apical and basolateral chambers at 24 h of exposure to IL-1β were not significantly different from the respective CINC-1 levels found at the 8-h time point. In dose-response studies, the cells were exposed to 0.01, 0.1, 1, and 10 ng/ml of IL-1β for 8 h (Figure 4B). A 32-fold increase in CINC-1 secretion over its constitutive production was induced by IL-1β at 10 pg/ml. Similar to control conditions, CINC-1 was largely released across the apical membrane of choroidal epithelium. The exposure of epithelial monolayers to IL-1β at 100 pg/ml resulted in a ~600-fold increase in CINC-1 production and the polarity of CINC-1 secretion was reversed, with approximately 2/3 of the chemokine produced by choroidal cells being secreted across the basolateral membrane. The production of CINC-1 reached a plateau when IL-1β was applied to epithelial monolayers at 1 ng/ml.

The possible effect of the leak and/or transcellular transfer of CXC chemokines on our estimates of polarity of CINC-1 secretion by epithelial monolayers was evaluated. To this end, the basolateral surface of the monolayers was exposed to conditioned media collected from IL-1β-treated cells. The monolayers were exposed for 1.5 h to the conditioned medium containing 513 pg/ml of CINC-1 and for 4 h when the medium contained 2.62 ng/ml of CINC-1. The levels of CINC-1 measured in the apical chamber at the end of the incubation periods were higher than those resulting from the constitutive secretion, which was assessed in parallel. However, the amounts of CINC-1 that actually permeated the monolayers represented only

0.53±0.13 to 0.57±0.10% of the amount of the chemokine present in the basolateral chamber. Similar low basolateral-to-apical permeability to CINC-1 was observed when the recombinant chemokine was applied at 0.4 and 4 ng/ml for 1.5 and 4 h, respectively (data not shown). The exposure of epithelial monolayers to IL-1β or CINC-1 did not cause any apparent alterations in the integrity of the BCSFB, as demonstrated by the lack of changes in paracellular permeability to sucrose (Figures 4C and 4D, data not shown).

Neutrophil trafficking across the BCSFB

Post-traumatic induction of choroidal synthesis of chemokines was followed by neutrophil recruitment to the ipsilateral CP; however, there was a significant delay between an increase in chemokine production and neutrophil accumulation in choroidal tissue (Figures 5A–5F). Neutrophils infiltrating the ipsilateral CP were found at 1 day after injury, whereas at 8 h post-TBI, these inflammatory cells were only sporadically observed to accumulate in the ipsilateral CP. This neutrophil influx was transient, as no neutrophils were found to infiltrate the ipsilateral CP at 2 days after TBI. Neutrophils did not accumulate in the contralateral CP (Figures 5A, 5C, and 5E), which was consistent with the absence of post-traumatic induction of CINC-1 synthesis in the contralateral CP and only a limited upregulation of expression of CINC-2α and CINC-3/MIP-2 observed in this tissue (see Figures 2A–2C). These immunohistochemical data were confirmed by the MPO activity assays. Low, but consistently detectable, MPO activity was found in the contralateral CP. It is likely that stromal macrophages and/or epiplexus cells contributed to this low MPO activity (Nagra *et al*, 1997). At 8 h post-TBI, there was a slight, but significant, increase in MPO activity in the ipsilateral CP when compared with the contralateral CP (Figure 5G). Consistent with immunohistochemical findings, MPO activity in the ipsilateral CP peaked at 1 day after injury. Interestingly, elevated MPO activity in the ipsilateral CP was also found at 2 days post-injury, which was likely associated with the accumulation of monocytes observed at that time point after TBI (unpublished observations). Similar pattern of changes in MPO activity was found in the cerebral cortex adjacent to the lesion, but the peak levels of MPO activity (at 1 day post-TBI) were ~5-fold higher than those observed in the ipsilateral CP (Figure 5H). MPO activity was undetectable in the contralateral cortex.

To demonstrate neutrophil trafficking across the BCSFB, we used TEM. The contralateral CP harvested at 1 d post-TBI had normal morphology (Figure 6A), similar to the morphology of choroidal tissue from sham-injured rats (data not shown). Choroidal epithelial cells had well-defined microvilli and the lateral membrane was folded into elaborate interdigitating processes near the base of the cells. The space between adjacent epithelial cells was narrow and the tight junctions between the cells were well discernible. In the ipsilateral CP, neutrophils were found to infiltrate the stroma and subsequently reach the intercellular space between epithelial cells (Figures 6B and 6C). The movement of neutrophils between epithelial cells toward their apical domain did not appear to affect the integrity of tight junctions.

Discussion

Brain injury is associated with a rapid and substantial increase in synthesis of proinflammatory cytokines, such as TNF-α and IL-1β, in traumatized brain parenchyma (Fan *et al*, 1995, 1996). Here we found that, after TBI, the expression of TNF-α and IL-1β is also upregulated in the CP located ipsilaterally to the injury. Therefore, an increase in CSF levels of proinflammatory cytokines observed in TBI patients (Singhal *et al*, 2002; Buttram *et al*, 2007) may result from production of these inflammatory mediators by both brain parenchymal cells and the choroidal tissue. Proinflammatory cytokines are strong inducers of epithelial synthesis of CXC chemokines (Takaishi *et al*, 2000; Handa *et al*, 2004), and we observed a gradual increase in choroidal expression of these chemokines after TBI. It is likely that CSF-

borne proinflammatory mediators, including TNF-α and IL-1β, play a major role in inducing the production of neutrophil chemoattractants in the CP, and that this choroidal chemokine production is, in part, augmented by CP-derived cytokines. Neutrophils themselves are also able to produce CXC chemokines and can respond with increased chemokine synthesis to inflammatory stimuli, such as lipopolysaccharide (Scapini *et al*, 2000). However, the post-traumatic increase in expression of CXC chemokines observed in the ipsilateral CP was not related to neutrophil accumulation in choroidal tissue. In fact, there was a considerable delay between an increase in choroidal synthesis of chemokines and neutrophil invasion of CP, and at 1 day post-TBI, when neutrophils infiltrated this tissue, the mRNA levels in the ipsilateral CP for all three chemokines studied were close to those found in the contralateral CP or in the CP from sham-injured rats. Interestingly, an increase in chemokine expression in both the ipsilateral CP and the ipsilateral cerebral cortex peaked at approximately the same time after injury (6 h post-TBI), but the time courses of neutrophil influx to these brain regions differed. Indeed, neutrophil invasion to the injured cortex was occasionally observed as early as 4 h after TBI and was consistently observed at 6–8 h post-injury (Chodobski *et al*, 2003), whereas in the CP, these inflammatory cells were only sporadically observed at 8 h post-TBI. These observations suggest that factors other than chemokine synthesis, such as for example different time courses of induction of expression of cell adhesion molecules on choroidal and cerebrovascular endothelium, account for different kinetics of neutrophil migration to the CP and traumatized brain parenchyma.

Specific targeting by neutrophils of ipsilateral CP located at some distance from the site of injury is unique. The recruitment of inflammatory cells to the CP has previously been observed after intraparenchymal injection of IL-1β, and it occurred in the absence of leukocyte influx to the site of injection (Andersson *et al*, 1992). It is likely that the volume-transmission-mediated signaling involving bulk flow of interstitial fluid (ISF) plays a critical role in choroidal induction of chemokine synthesis and resultant recruitment of neutrophils (Redzic *et al*, 2005). Volume transmission may also play a role in post-traumatic increase in expression of proinflammatory mediators observed in the contralateral CP and contralateral hippocampus (data not shown). Consistent with this idea, unilateral injury to the cerebral cortex has been found to promote bulk flow of ISF along the white matter fibers of corpus callosum from the ipsilateral to contralateral hemisphere (Kamada *et al*, 1995). We have also observed an increase in chemokine synthesis in the 4th ventricle CP, although the levels of expression of these inflammatory mediators in this tissue were lower than those found in the lateral ventricle CP ipsilateral to injury (data not shown). As CSF flows from the lateral ventricles to the 3rd ventricle and thereafter continues its movement along the cerebral aqueduct and the 4th ventricle, the induction of chemokine synthesis in the 4th ventricle CP was likely mediated by volume transmission involving bulk flow of CSF (Redzic *et al*, 2005). Despite increased chemokine synthesis, in neither the 4th ventricle CP nor the CP from the lateral ventricle contralateral to injury was neutrophil recruitment observed. It is possible that, in these tissues, the levels of expression of CXC chemokines were too low and/or there was insufficient induction of expression of cell adhesion molecules on choroidal microvasculature to promote neutrophil migration.

To characterize the inducibility and direction of chemokine release from the choroidal epithelium, we used an *in vitro* model of the BCSFB (Strazielle and Ghersi-Egea, 1999). The functional polarization of choroidal epithelium in this BCSFB model has previously been ascertained by evaluating the efflux of glucurono-conjugates and secretion of matrix metalloproteinases, which demonstrated similar polarity in both the *in vitro* model and in *ex vivo* freshly isolated CP (Strazielle and Ghersi-Egea, 1999; Strazielle *et al*, 2003). A significant increase in CINC-1 secretion above the control levels was observed in response to IL-1β at a concentration as low as 10 pg/ml, which is comparable with the levels of IL-1β found in the CSF of TBI patients (Singhal *et al*, 2002; Buttram *et al*, 2007). CINC-1 secretion was increased

further in response to higher concentrations of IL-1β. Using an *in vitro* model of the BCSFB, we have also demonstrated that CXC chemokines are secreted across both the apical (CSF-facing) and basolateral (stroma/blood-facing) membranes of choroidal epithelium. The permeability of epithelial monolayers to CINC-1, while detectable, was low and therefore did not affect the polarity of chemokine secretion observed in response to IL-1β.The paracellular permeability of epithelial monolayers to the low-molecular marker was also low and was not affected by the exposure to IL-1β or CINC-1, which further validates our estimates of polarity of chemokine secretion. Our findings are in line with the previous studies, where bidirectional chemokine secretion by intestinal epithelia has been demonstrated and found to be necessary for neutrophil migration across this epithelial barrier (McCormick *et al*, 1995, 1998).

The above-discussed features of choroidal epithelium, such as the ability to synthesize CXC chemokines in response to injury and bidirectional secretion of these chemokines across theapical and basolateral membranes of choroidal epithelial cells, strongly suggest that the BCSFB plays a role in post-traumatic invasion of neutrophils. This idea is further supported by our TEM analysis of choroidal tissue. Similar to the movement across the BBB (Wong *et al*, 2007), the migration of neutrophils across the BCSFB was found to involve the paracellular pathway and did not appear to affect the integrity of tight junctions.

Acknowledgments

References

Andersson PB, Perry VH, Gordon S. Intracerebral injection of proinflammatory cytokines or leukocyte chemotaxins induces minimal myelomonocytic cell recruitment to the parenchyma of the central nervous system. J Exp Med 1992;176:255–9. [PubMed: 1613459]

Beech JS, Reckless J, Mosedale DE, Grainger DJ, Williams SC, Menon DK. Neuroprotection in ischemia-reperfusion injury: an antiinflammatory approach using a novel broad-spectrum chemokine inhibitor. J Cereb Blood Flow Metab 2001;21:683–9. [PubMed: 11488537]

Bloom GS, Brashear TA. A novel 58-κDa protein associates with the Golgi apparatus and microtubules. J Biol Chem 1989;264:16083–92. [PubMed: 2777777]

Buttram SD, Wisniewski SR, Jackson EK, Adelson PD, Feldman K, Bayir H, Berger RP, Clark RS, Kochanek PM. Multiplex assessment of cytokine and chemokine levels in cerebrospinal fluid following severe pediatric traumatic brain injury: effects of moderate hypothermia. J Neurotrauma 2007;24:1707–17. [PubMed: 18001201]

Carlos TM, Clark RS, Franicola-Higgins D, Schiding JK, Kochanek PM. Expression of endothelial adhesion molecules and recruitment of neutrophils after traumatic brain injury in rats. J Leukoc Biol 1997;61:279–85. [PubMed: 9060450]

Chodobski A, Chung I, KoŸniewska E, Ivanenko T, Chang W, Harrington JF, Duncan JA, Szmydynger-Chodobska J. Early neutrophilic expression of vascular endothelial growth factor after traumatic brain injury. Neuroscience 2003;122:853–67. [PubMed: 14643756]

Ericsson A, Liu C, Hart RP, Sawchenko PE. Type 1 interleukin-1 receptor in the rat brain: distribution, regulation, and relationship to sites of IL-1-induced cellular activation. J Comp Neurol 1995;361:681–98. [PubMed: 8576422]

Fan L, Young PR, Barone FC, Feuerstein GZ, Smith DH, McIntosh TK. Experimental brain injury induces expression of interleukin-1β mRNA in the rat brain. Mol Brain Res 1995;30:125–30. [PubMed: 7609633]

Fan L, Young PR, Barone FC, Feuerstein GZ, Smith DH, McIntosh TK. Experimental brain injury induces differential expression of tumor necrosis factor-α mRNA in the CNS. Mol Brain Res 1996;36:287–91. [PubMed: 8965649]

Fayein NA, Courtois Y, Jeanny JC. Basic fibroblast growth factor high and low affinity binding sites in developing mouse brain, hippocampus and cerebellum. Biol Cell 1992;76:1–13. [PubMed: 1294285]

Handa O, Naito Y, Takagi T, Shimozawa M, Kokura S, Yoshida N, Matsui H, Cepinskas G, Kvietys PR, Yoshikawa T. Tumor necrosis factor-α-induced cytokine-induced neutrophil chemoattractant-1 (CINC-1) production by rat gastric epithelial cells: role of reactive oxygen species and nuclear factor-κB. J Pharmacol Exp Ther 2004;309:670–6. [PubMed: 14747614]

Huang S, Paulauskis JD, Godleski JJ, Kobzik L. Expression of macrophage inflammatory protein-2 and KC mRNA in pulmonary inflammation. Am J Pathol 1992a;141:981–8. [PubMed: 1415488]

Huang S, Paulauskis JD, Kobzik L. Rat KC cDNA cloning and mRNA expression in lung macrophages and fibroblasts. Biochem Biophys Res Commun 1992b;184:922–9. [PubMed: 1374243]

Kamada K, Houkin K, Hida K, Iwasaki Y, Abe H. Serial changes in metabolism and histology in the cold-injury trauma rat brain model. Proton magnetic resonance imaging and spectroscopy study. Neurol Med Chir (Tokyo) 1995;35:1–7. [PubMed: 7700475]

Kivisäkk P, Mahad DJ, Callahan MK, Trebst C, Tucky B, Wei T, Wu L, Baekkevold ES, Lassmann H, Staugaitis SM, Campbell JJ, Ransohoff RM. Human cerebrospinal fluid central memory CD4$^+$ T cells: evidence for trafficking through choroid plexus and meninges via P-selectin. Proc Natl Acad Sci USA 2003;100:8389–94. [PubMed: 12829791]

Kobayashi Y. The role of chemokines in neutrophil biology. Front Biosci 2008;13:2400–7. [PubMed: 17981721]

Kriegler M, Perez C, DeFay K, Albert I, Lu SD. A novel form of TNF/cachectin is a cell surface cytotoxic transmembrane protein: ramifications for the complex physiology of TNF. Cell 1988;53:45–53. [PubMed: 3349526]

Kuschert GS, Coulin F, Power CA, Proudfoot AE, Hubbard RE, Hoogewerf AJ, Wells TN. Glycosaminoglycans interact selectively with chemokines and modulate receptor binding and cellular responses. Biochemistry 1999;38:12959–68. [PubMed: 10504268]

Ling EA, Kaur C, Lu J. Origin, nature, and some functional considerations of intraventricular macrophages, with special reference to the epiplexus cells. Microsc Res Tech 1998;41:43–56. [PubMed: 9550136]

Magnoni S, Stocchetti N, Colombo G, Carlin A, Colombo A, Lipton JM, Catania A. α-Melanocyte-stimulating hormone is decreased in plasma of patients with acute brain injury. J Neurotrauma 2003;20:251–60. [PubMed: 12820679]

Matsumoto T, Ikeda K, Mukaida N, Harada A, Matsumoto Y, Yamashita J, Matsushima K. Prevention of cerebral edema and infarct in cerebral reperfusion injury by an antibody to interleukin-8. Lab Invest 1997;77:119–25. [PubMed: 9274853]

McCormick BA, Hofman PM, Kim J, Carnes DK, Miller SI, Madara JL. Surface attachment of *Salmonella typhimurium* to intestinal epithelia imprints the subepithelial matrix with gradients chemotactic for neutrophils. J Cell Biol 1995;131:1599–608. [PubMed: 8522615]

McCormick BA, Parkos CA, Colgan SP, Carnes DK, Madara JL. Apical secretion of a pathogen-elicited epithelial chemoattractant activity in response to surface colonization of intestinal epithelia by *Salmonella typhimurium*. J Immunol 1998;160:455–66. [PubMed: 9552004]

Nadeau S, Rivest S. Effects of circulating tumor necrosis factor on the neuronal activity and expression of the genes encoding the tumor necrosis factor receptors (p55 and p75) in the rat brain: a view from the blood-brain barrier. Neuroscience 1999;93:1449–64. [PubMed: 10501470]

Nagra RM, Becher B, Tourtellotte WW, Antel JP, Gold D, Paladino T, Smith RA, Nelson JR, Reynolds WF. Immunohistochemical and genetic evidence of myeloperoxidase involvement in multiple sclerosis. J Neuroimmunol 1997;78:97–107. [PubMed: 9307233]

Nakagawa H, Komorita N, Shibata F, Ikesue A, Konishi K, Fujioka M, Kato H. Identification of cytokine-induced neutrophil chemoattractants (CINC), rat GRO/CINC-2α and CINC-2β, produced by granulation tissue in culture: purification, complete amino acid sequences and characterization. Biochem J 1994;301:545–50. [PubMed: 8043001]

Praetorius J, Nielsen S. Distribution of sodium transporters and aquaporin-1 in the human choroid plexus. Am J Physiol 2006;291:C59–C67.

Quan N, Stern EL, Whiteside MB, Herkenham M. Induction of pro-inflammatory cytokine mRNAs in the brain after peripheral injection of subseptic doses of lipopolysaccharide in the rat. J Neuroimmunol 1999;93:72–80. [PubMed: 10378870]

Redzic ZB, Preston JE, Duncan JA, Chodobski A, Szmydynger-Chodobska J. The choroid plexus-cerebrospinal fluid system: from development to aging. Curr Top Dev Biol 2005;71:1–52. [PubMed: 16344101]

Scapini P, Lapinet-Vera JA, Gasperini S, Calzetti F, Bazzoni F, Cassatella MA. The neutrophil as a cellular source of chemokines. Immunol Rev 2000;177:195–203. [PubMed: 11138776]

Schoettle RJ, Kochanek PM, Magargee MJ, Uhl MW, Nemoto EM. Early polymorphonuclear leukocyte accumulation correlates with the development of posttraumatic cerebral edema in rats. J Neurotrauma 1990;7:207–17. [PubMed: 2127947]

Singhal A, Baker AJ, Hare GM, Reinders FX, Schlichter LC, Moulton RJ. Association between cerebrospinal fluid interleukin-6 concentrations and outcome after severe human traumatic brain injury. J Neurotrauma 2002;19:929–37. [PubMed: 12225653]

Snow AD, Sekiguchi RT, Nochlin D, Kalaria RN, Kimata K. Heparan sulfate proteoglycan in diffuse plaques of hippocampus but not of cerebellum in Alzheimer's disease brain. Am J Pathol 1994;144:337–47. [PubMed: 8311117]

Strazielle N, Ghersi-Egea JF. Demonstration of a coupled metabolism-efflux process at the choroid plexus as a mechanism of brain protection toward xenobiotics. J Neurosci 1999;19:6275–89. [PubMed: 10414957]

Strazielle N, Ghersi-Egea JF. Choroid plexus in the central nervous system: biology and physiopathology. J Neuropathol Exp Neurol 2000;59:561–74. [PubMed: 10901227]

Strazielle N, Khuth ST, Murat A, Chalon A, Giraudon P, Belin MF, Ghersi-Egea JF. Pro-inflammatory cytokines modulate matrix metalloproteinase secretion and organic anion transport at the blood-cerebrospinal fluid barrier. J Neuropathol Exp Neurol 2003;62:1254–64. [PubMed: 14692701]

Strazielle N, Preston JE. Transport across the choroid plexuses in vivo and in vitro. Methods Mol Med 2003;89:291–304. [PubMed: 12958428]

Takaishi K, Ohtsuka T, Tsuneyoshi S, Maehara N, Harada M, Yoshida H, Watanabe K, Tsurufuji S. Inhibition of the production of rat cytokine-induced neutrophil chemoattractant (CINC)-1, a member of the interleukin-8 family, by adenovirus-mediated overexpression of IκBα. J Biochem 2000;127:511–6. [PubMed: 10731724]

Wong D, Prameya R, Dorovini-Zis K. Adhesion and migration of polymorphonuclear leukocytes across human brain microvessel endothelial cells are differentially regulated by endothelial cell adhesion molecules and modulate monolayer permeability. J Neuroimmunol 2007;184:136–48. [PubMed: 17291598]

Yamasaki Y, Matsuo Y, Zagorski J, Matsuura N, Onodera H, Itoyama Y, Kogure K. New therapeutic possibility of blocking cytokine-induced neutrophil chemoattractant on transient ischemic brain damage in rats. Brain Res 1997;759:103–11. [PubMed: 9219868]
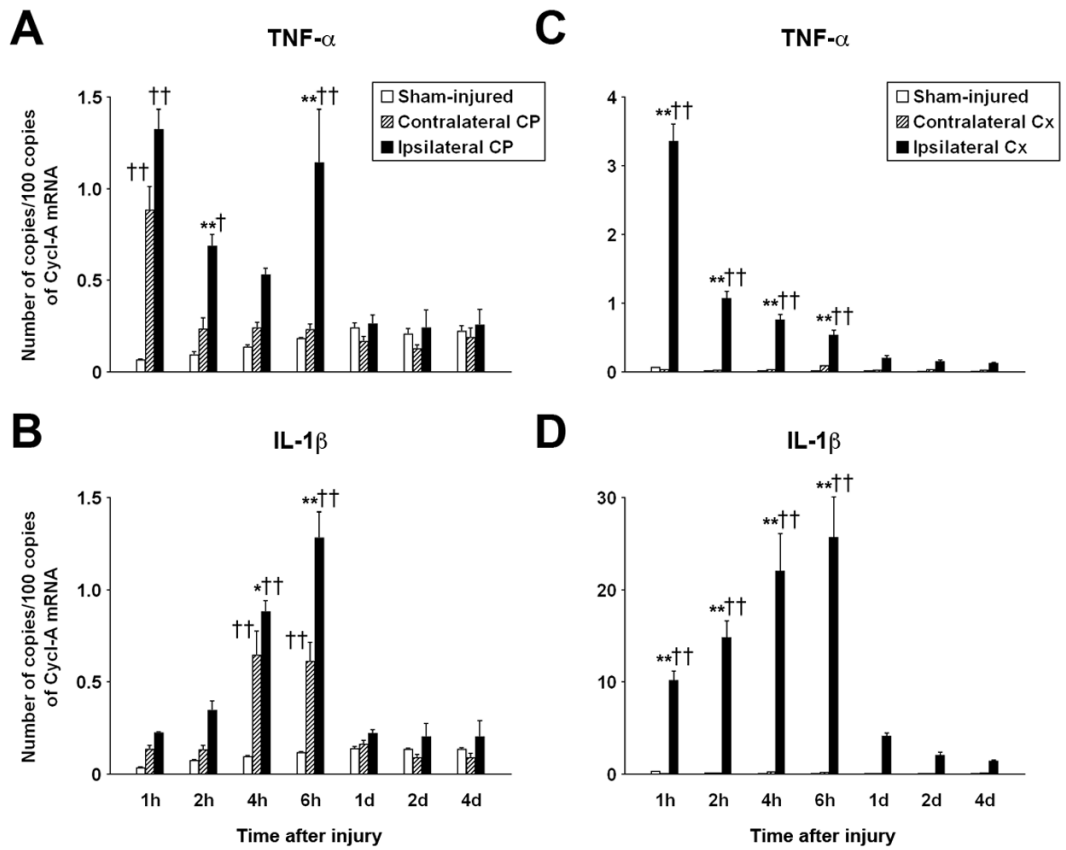
Figure 1.
Real-time RT-PCR analysis of temporal changes in choroidal (CP) and cortical (Cx) expression of TNF-α and IL-1β after TBI. The controlled cortical impact model of TBI in rats was used. (**A**, **B**) Changes in mRNA for TNF-α and IL-1β, respectively, in the ipsilateral and contralateral CPs, and in the CP from sham-injured rats ($n=9$–10 rats per time point). (**C**, **D**) Changes in mRNA for TNF-α and IL-1β, respectively, in the cerebral cortex ($n=6$ rats per time point). The number of copies of transcripts for each cytokine relative to the message for cyclophilin A (Cycl-A) is shown. Data represent mean values ± SEM. *$P<0.05$, **$P<0.01$ for the ipsilateral CP/Cx vs. contralateral CP/Cx (Newman-Keuls test). †$P<0.05$, ††$P<0.01$ for the ipsilateral or contralateral CP/Cx vs. the CP/Cx from sham-injured rats (Newman-Keuls test).
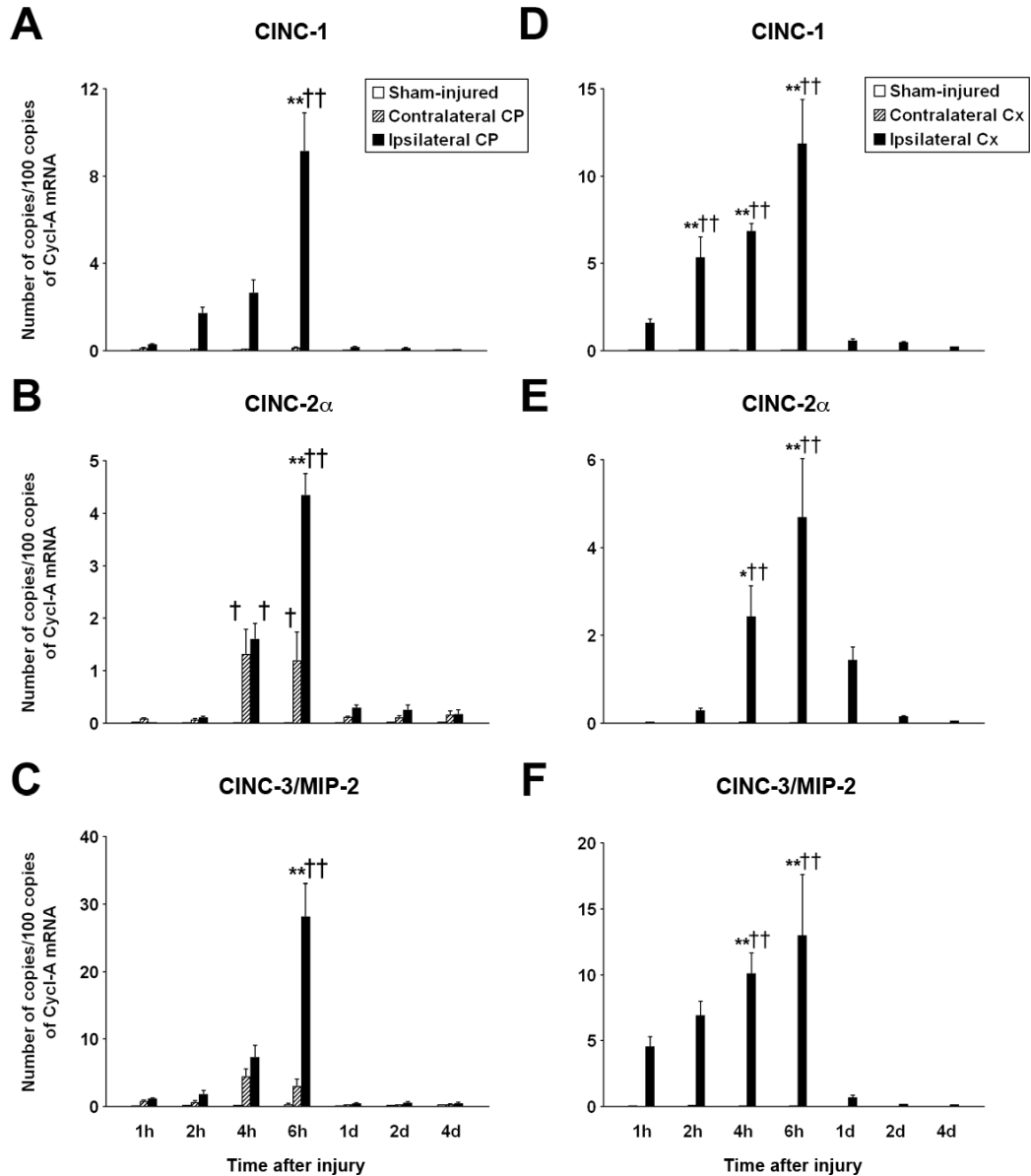
Figure 2.
Real-time RT-PCR analysis of post-traumatic changes in choroidal (CP) and cortical (Cx) expression of neutrophil chemoattractants. (**A**, **B**, **C**) Changes in mRNA for CINC-1, CINC-2α, and CINC-3/MIP-2, respectively, in the ipsilateral and contralateral CPs, and in the CP from sham-injured rats (n=9–10 animals per time point). (**D**, **E**, **F**) Changes in mRNA for TNF-α and IL-1β, respectively, in the cerebral cortex (n=6 rats per time point). The number of copies of transcripts for each chemokine relative to the message for cyclophilin A (Cycl-A) is shown. Data represent mean values ± SEM. *P<0.05, **P<0.01 for the ipsilateral CP/Cx vs. contralateral CP/Cx (Newman-Keuls test). †P<0.05, ††P<0.01 for the ipsilateral or contralateral CP/Cx vs. the CP/Cx from sham-injured rats (Newman-Keuls test).
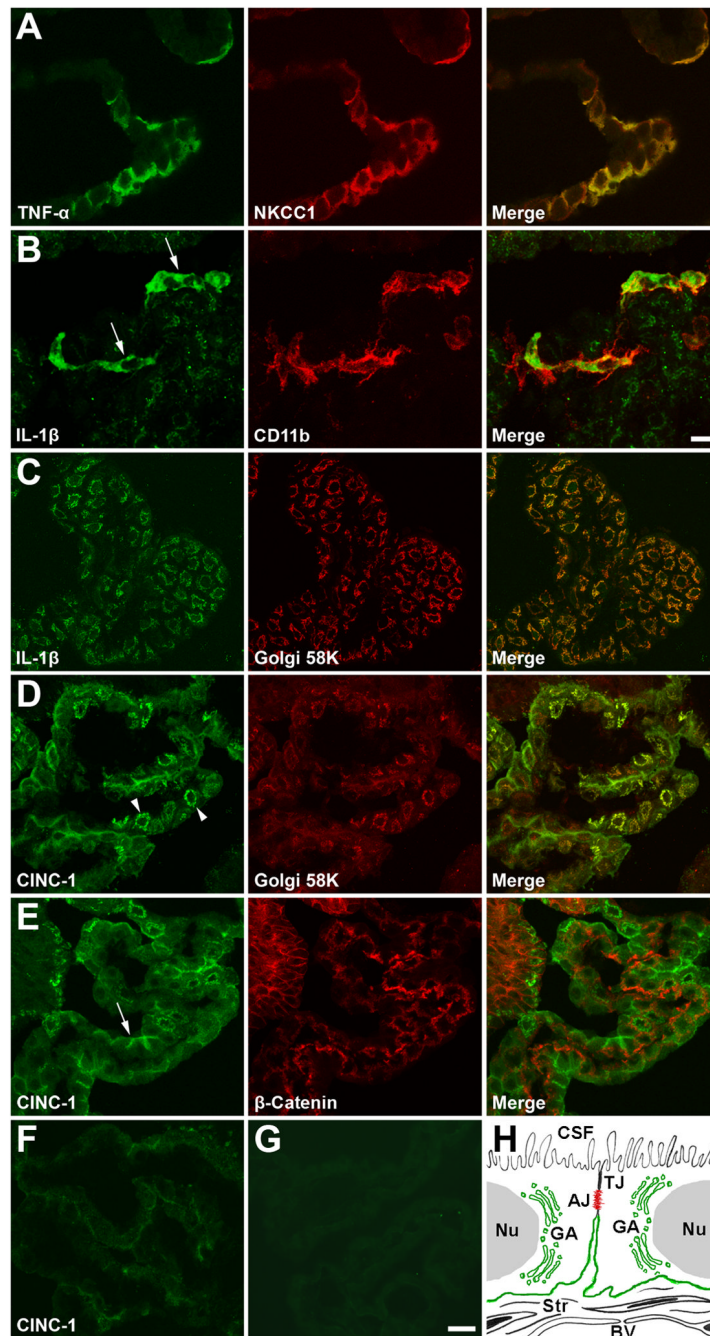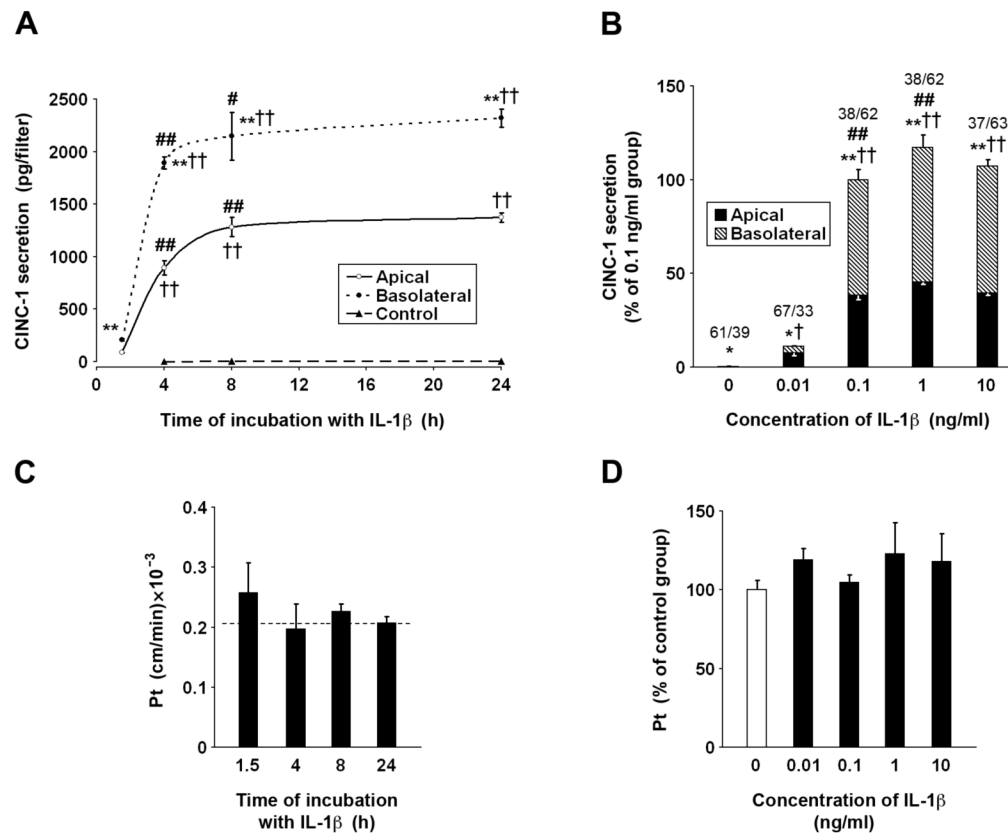
Figure 3.
Immunohistochemical localization of TNF-α, IL-1β, and CINC-1 in the lateral ventricle CP.
Confocal microscopy images of choroidal tissue harvested at 8 h post-TBI are shown. (**A**)
Double staining of the ipsilateral CP with anti-TNF-α antibody and the antibody to the apically
expressed marker, the NKCC1 co-transporter. (**B**) The ipsilateral CP. Localization of the
IL-1β-immunoreactive product to epiplexus (Kolmer) cells (arrows) stained with the antibody
to CD11b, an antigen expressed on macrophages and other inflammatory cells. (**C**) Double
staining of the ipsilateral CP with anti-IL-1β antibody and the antibody to the Golgi marker,
Golgi 58K. Similar pattern of IL-1β-immunopositive staining was found in the contralateral
CP and in the choroidal tissue from sham-injured rats. (**D**) Double staining of the ipsilateral

CP with anti-CINC-1 antibody and the antibody to Golgi 58K. The localization of CINC-1 to the Golgi complex (arrowheads) is consistent with increased synthesis of this secreted protein occurring after TBI. (**E**) Localization of the CINC-1-immunoreactive product to the basolateral membrane of epithelial cells in the ipsilateral CP (arrows). Note that the basolateral CINC-1 staining does not co-localize with the staining for β-catenin, a component of the adherens junction complex, indicating that CINC-1 is confined to a part of the basolateral membrane that is distinct from areas occupied by adherens junctions (see **H**). (**F**) A weak basolateral staining for CINC-1 in the contralateral CP. This pattern of staining was similar to that found in the choroidal tissue from sham-injured rats. (**G**) Negative control staining. In these experiments, the brain sections were incubated with anti-CINC-1 antibody that had been pre-absorbed overnight with recombinant rat CINC-1 at 100 μg/ml. The ipsilateral CP is shown. Bars: **A**, **C–G**, 20 μm; **B**, 10 μm. (**H**) Schematic representation of CINC-1 localization in choroidal tissue. AJ, adherens junction; BV, blood microvessel; CSF, cerebrospinal fluid; GA, Golgi apparatus; Nu, nucleus; Str, choroidal stroma; TJ, tight junction.

Figure 4.
Secretion of CINC-1 in primary cell cultures of rat choroidal epithelial cells. The cells were seeded on Transwell Clear inserts as described in *Materials and methods*. The experiments were performed 5 days after the cells reached confluence (*n*=3–6 per group). The apical surface of epithelial monolayers was exposed to IL-1β and the concentration of CINC-1 in the apical and basolateral chambers was quantified by ELISA. (**A**) The time-course studies. The cells were incubated with 0.1 ng/ml of IL-1β for up to 24 h. During the initial 4-h period ofexposure to IL-1β, the CINC-1 levels in the apical and basolateral chambers increased rapidly; however, between 4 and 8 h of incubation with this cytokine, the CINC-1 levels increased at much slower rate. (**B**) The dose-response studies. The cells were exposed to IL-1β for 8 h. The fractions above the columns represent the proportion (%) of apical vs. basolateral release of CINC-1 to the culture media. Under control conditions, CINC-1 was constitutively produced, but it was barely detectable, and the total amount of CINC-1 secreted to the apical and basolateral chambers during the 8-h observation period was ~6 pg/filter. This secretion was polarized, with CINC-1 being predominantly released across the apical (CSF-facing) membrane. Note that the exposure of epithelial monolayers to IL-1β at 0.1 ng/ml resulted in a large increase in CINC-1 synthesis, but the polarity of CINC-1 secretion was reversed and an approximately 2/3 of the chemokine produced by choroidal cells was secreted across the basolateral (stroma/blood-facing) membrane. All data represent mean values ± SD. *$P<0.05$, **$P<0.01$ for apical vs. basolateral CINC-1 secretion (Student's *t* test with Bonferroni correction). [†]$P<0.05$, [††]$P<0.01$ for CINC-1 secretion in response to IL-1β vs. control (Dunnett test). [#]$P<0.05$, [##]$P<0.01$ for a difference in CINC-1 secretion at two consecutive time points during the exposure to IL-1β or in response to a 10-fold increase in IL-1β concentration (Tukey-Kramer test). The integrity of epithelial monolayers exposed to IL-1β was examined by measuring the permeability of each filter to the paracellular permeability marker ^{14}C-sucrose

(*n*=3–6 per group). The permeability $\times$ surface area product, PSt, was calculated from the ^{14}C-sucrose clearance rates as described in *Materials and methods*. The permeability coefficient, Pt, was calculated by dividing PSt by the surface area of the cell monolayer. (**C**) Temporal changes in paracellular permeability during the exposure to 0.1 ng/ml of IL-1β. The dashed line represents the Pt value obtained in untreated cells. (**D**) Changes in paracellular permeability in response to varying concentrations of IL-1β during the 8-h incubation with the cytokine. No statistically significant differences were observed among the groups.
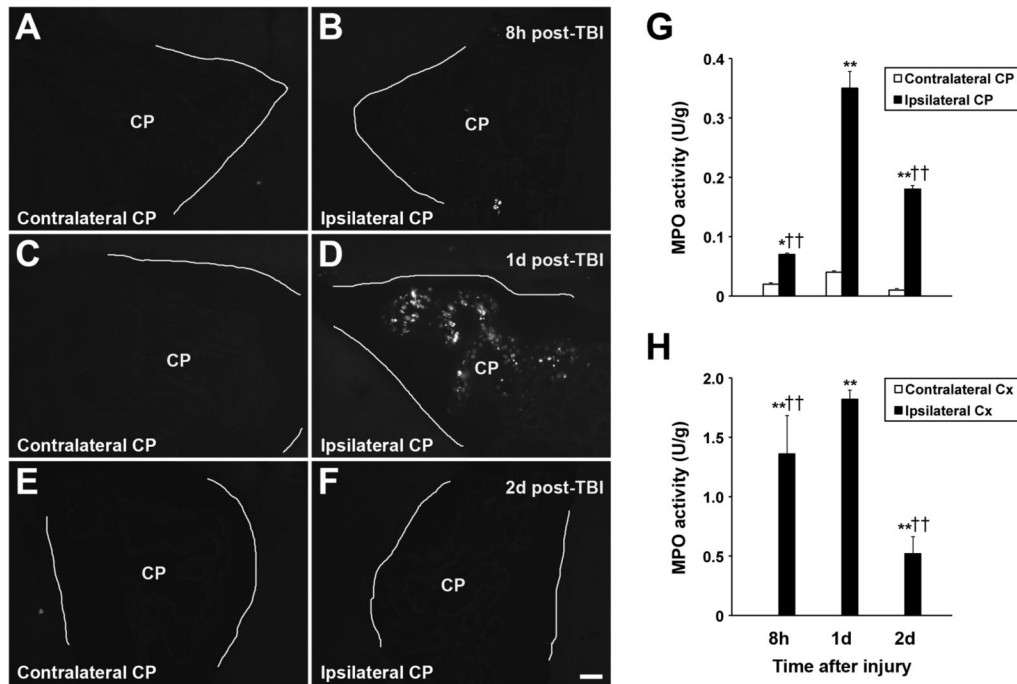
Figure 5.
Post-traumatic accumulation of neutrophils in the CP. (**A**, **C**, **E**) Low-power microphotographs of the contralateral CP at 8, 24, and 48 h post-TBI, respectively. (**B**, **D**, **F**) The ipsilateral CP at 8, 24, and 48 h post-TBI, respectively. The walls of the lateral ventricles are outlined. Neutrophils were detected by immunohistochemistry with anti-MPO antibody. Note that there was a significant delay between an increase in choroidal synthesis of chemokines and neutrophil accumulation in choroidal tissue. Neutrophils infiltrating the ipsilateral CP were found at 1 day after injury, whereas at 8 h post-TBI, these inflammatory cells were only sporadically observed to accumulate in the ipsilateral CP. This neutrophil influx was transient, as no neutrophils were found to infiltrate the ipsilateral CP at 2 days after TBI. Neutrophils did not accumulate in the contralateral CP. Bar: 50 μm. (**G**) The time course of post-traumatic changes in MPO activity in the CP (n=4 rats per time point). Low, but consistently detectable, MPO activity was found in the contralateral CP, which was likely associated with stromal macrophages and/or epiplexus cells normally present in the choroidal tissue. (**H**) Changes in MPO activity in the cerebral cortex adjacent to the lesion (n=4 rats per time point). Note that the peak levels (at 1 day post-TBI) of MPO activity in the injured cortex were ~5-fold higher than those observed in the ipsilateral CP. MPO activity was undetectable in the contralateral cortex. Data represent mean values ± SD. *P<0.05, **P<0.01 for the ipsilateral CP/Cx vs. contralateral CP/Cx (Newman-Keuls test). ††P<0.01 for the ipsilateral CP/Cx vs. the ipsilateral CP/Cx at 1 day post-TBI (Newman-Keuls test).
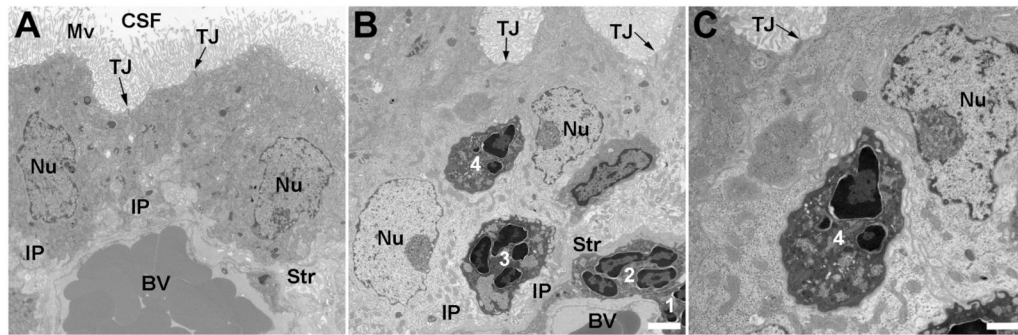
Figure 6.

Transmission electron microscopy (TEM) analysis of the CP. The choroidal tissue was harvested at 1 day after TBI and processed for TEM. (**A**) The contralateral CP, which has normal morphology, similar to the morphology of choroidal tissue from sham-injured rats (data not shown). Note that the choroidal epithelial cells have well-defined microvilli and the lateral membrane is folded into elaborate interdigitating processes near the base of the cells. The space between adjacent epithelial cells is narrow and the tight junctions between the cells are well discernible. (**B**) The ipsilateral CP. The microphotograph shows neutrophils (1 and 2) that extravasated into the choroidal stroma and those (3 and 4) that reached the intercellular space between choroidal epithelial cells. The movement of neutrophils between epithelial cells toward their apical domain does not appear to affect the integrity of tight junctions. (**C**) A higher magnification view of neutrophil 4 migrating between choroidal epithelial cells. Bars: **A**, **B**, 2 μm; **C**, 1 μm. BV, blood microvessel; CSF, cerebrospinal fluid; IP, interdigitating processes; Mv, microvilli; Nu, nucleus of choroidal epithelial cell; Str, choroidal stroma; TJ, tight junction.

Table 1

The sequences of primers and TaqMan probes, and the predicted sizes of PCR products

Gene	Primer/probe	Sequence	Predicted size of PCR product (base pairs)
CINC-1	[a] F	5′-TGTCCAAAAGATGCTAAAGGG-3′	89
	R	5′-AGAAGCCAGCGTTCACCA-3′	
	P	5′-AAGATAGATTGCACCGATGGCGTC-3′	
CINC-2α	F	5′-CCAGAAGTTACTGAAGAGTGACAAG-3′	131
	R	5′-CAGGCAGAGGCTCATCCA-3′	
	P	5′-TGTACGGTGATGGAGGACCTGCC-3′	
CINC-3/MIP-2	F	5′-CTGAACAAAGGCAAGGCTAAC-3′	120
	R	5′-CATCAGGTACGATCCAGGCT-3′	
	P	5′-CCTGGAAAGGAAGAACATGGGCTC-3′	
TNF-α	F	5′-ATTTCCAACAACTACGATGCTC-3′	112
	R	5′-GAGTTCCGAAAGCCCATTG-3′	
	P	5′-CTGGATTGCGGGCTGCTCAT-3′	
IL-1β	F	5′-CTCAATGGACAGAACATAAGCC-3′	143
	R	5′-GGTGTGCCGTCTTTCATCA-3′	
	P	5′-AGAGACAAGCAACGACAAAATCCCTG-3′	
Cyclophilin A	F	5′-GGTGAAAGAAGGCATGAGCA-3′	152
	R	5′-GCTACAGAAGGAATGGTTTGATG-3′	
	P	5′-TTTGGGTCCAGGAATGGCAAGAC-3′	

[a]F, forward primer; R, reverse primer; P, probe.